Pharm Res (2015) 32:500–515
DOI 10.1007/s11095-014-1478-0

RESEARCH PAPER

The Effect of Polymeric Excipients on the Physical Properties and Performance of Amorphous Dispersions: Part I, Free Volume and Glass Transition

Jinjiang Li • Junshu Zhao • Li Tao • Jennifer Wang • Vrushali Waknis • Duohai Pan • Mario Hubert • Krishnaswamy Raghavan • Jatin Patel

Received: 6 June 2014 / Accepted: 25 July 2014 / Published online: 9 August 2014
© Springer Science+Business Media New York 2014

ABSTRACT

Purpose To investigate the structural effect of polymeric excipients on the behavior of free volume of drug-polymer dispersions in relation to glass transition.

Methods Two drugs (indomethacin and ketoconazole) were selected to prepare amorphous dispersions with PVP, PVPVA, HPC, and HPMCAS through spray drying. The physical attributes of the dispersions were characterized using SEM and PXRD. The free volume (hole-size) of the dispersions along with drugs and polymers was measured using positron annihilation lifetime spectroscopy (PALS). Their glass transition temperatures (Tgs) were determined using DSC and DMA. FTIR spectra were recorded to identify hydrogen bonding in the dispersions.

Results The chain structural difference-flexible (PVP and PVPVA) *vs.* inflexible (HPC and HPMCAS)-significantly impacts the free volume and Tgs of the dispersions as well as their deviation from ideality. Relative to Tg, free volume seems to be a better measure of hydrogen bonding interaction for the dispersions of PVP, HPC, and HPMCAS. The free volume of polymers and their dispersions in general appears to be related to their conformations in solution.

Conclusions Both the backbone chain rigidity of polymers as well as drug-polymer interaction can impact the free volume and glass transition behaviors of the dispersions.

J. Li (✉) • J. Zhao • L. Tao • J. Wang • V. Waknis • D. Pan • K. Raghavan • J. Patel
Drug Product Science and Technology, Bristol-Myers Squibb
New Brunswick, NJ, USA
e-mail: jinjiang.li@bms.com

M. Hubert
Analytical and Bioanalytical Development, Bristol-Myers Squibb
New Brunswick, NJ, USA

J. Wang
Teva Pharmaceuticals, North Wales, PA 19454, USA

KEY WORDS amorphous dispersions · chain rigidity and solution comformation · free volume by PALS · glass transition · polymeric excipients: cellulose derivatives and ploy vinyl polymers

INTRODUCTION

In the pharmaceutical industry, the development of oral solid dosage forms containing amorphous active pharmaceutical ingedients (APIs), for the purpose of improving bioavailability, still poses significant challenges, especially due to physical instability [1, 2]., To enhance the stability of amorphous APIs and their dissolution, the amorphous solid dispersions (ASDs) of APIs are often prepared using polymers, particularly spray dried dispersions to support both toxicological investigations and exploratory clinical studies, where there is a need to drive exposures to carefully assess safety [3]. This is due to the fact that molecules in amorphous state are less stable (higher energetic) compared to a crystalline solid. Hence, polymers can be used to mix with APIs to increase their Tgs and alter their interaction with water, consequently improving their physical stability and performance [4]. The amount of polymer in typical ASDs is often more than 50% (w/w). Therefore, the nature and type of the polymer used-a key component-could be a determining factor affecting the physical properties of ASDs. Specifically, polymers influence the physical stability of ASDs in relation to API crystallization as well as drug release in dissolution [5]. In the pharmaceutical industry, the polymers commonly used for preparing ASDs include the polyvinyl based synthetic polymers (*e.g.*, poly (vinyl pyrrolidone) (PVP) and poly (1-vinylpyrrolidone-*co*-vinyl acetate) (PVPVA)) as well as the derivatives of cellulose (hydroxypropyl cellulose (HPC) and hydroxylpropyl methylcellulose acetate succinate (HPMCAS) [6]. Their structural features are shown in Fig. 1. In particular, HPMCAS becomes the polymer of choice to prepare ASDs due to its properties of

improving physical stability, dissolution, and consequently bioavailability [7–10].

Although polymers are frequently used in preparing ASDs, the mechanism of the polymeric stabilization of drugs against crystallization as well as the enhancement of their dissolution are still not well understood. Historically, the inhibition of crystallization of indomethacin (IMC) by PVP was first reported by Matsumoto and Zografi, and the formation of hydrogen bonding between PVP and IMC was suggested as the stabilization mechanism based on vibrational spectroscopic evidence [11, 12]. In addition, for the dispersions of HPMCAS based, a speciation hypothesis was proposed by researchers from Capsulgel, Inc. (formerly Bend Research) [1]. Recently, the impact of polymers on the properties of ASDs, including the inhibition of API crystallization and the enhancement of dissolution by maintaining a super-saturation state, has been investigated by several research groups [13–16]. Nevertheless, the focus of these works was primarily towards monitoring the inhibition of API crystallization by polymers as well as the maintenance of supersaturation, but not on the impact of the structural differences of polymers on the physical properties of ASDs. As displayed in Fig. 1, polyvinyl based polymers (PVP (a) and PVPVA (b)) have backbones of carbon-carbon linkages, rendering their chains to be flexible, and thus their conformations in solution are Gaussian-like. However cellulose derivatives (HPC (c) and HPMCAS (d)) have rigid backbones of pyranosic ring (D-glucose group), and therefore they exhibit a semi-flexible (worm-like) chain behavior in solution [17, 18]. These structural differences can impact the physical properties of ASDs such as free volume and glass transition as demonstrated in this paper. In addition, since PVPVA is a copolymer of vinyl pyrrolidone with vinyl acetate, its solution and solid state behaviors are dominated by the balance of hydrophilic-hydrophobic properties [19].

Glass transition temperature (Tg), which is closely related to the change of free volume-the difference between the specific volume and the occupied volume-in amorphous phases, is an important indicator of API physical stability against crystallization in ASDs. Tg represents the point where the specific volume undergoes a discontinuity with temperature; at glass transition, a glassy phase has the same free volume (iso-free volume, 2.5%) as its liquid/rubbery phase [20]. Historically, the concept of free volume was originally proposed by Doolittle, and it was further developed by Cohen and Turnbull, based on the following assumptions: (1) there is no diffusion in amorphous phases if all of the available free volume (existing as holes or vacancies) is smaller than the critical value (v^*) for "molecular jumps" to occur (no cooperative reorganization);(2) when micro-Brownian motion and thermal fluctuation create a hole greater than v^*, molecular diffusion starts [21]. According to the redistribution of free volume, Cohen and Turnbull described the diffusion of molecules in the liquid or amorphous phase as:

$$\langle D\rangle = D(v^*)exp\left(-\frac{\gamma v^*}{v_{free,\ average}}\right) \quad (1)$$

where $D(v^*)$, γ, v^*, and $v_{free,\ average}$ are the diffusion coefficient at the critical free volume, a cell-cell overlap factor, the critical free volume, and the average free volume at a state, respectively [21]. Typically, diffusion coefficients are higher at higher temperatures because, on average, the free volume per lattice cell increases with temperature. For amorphous drug-polymer dispersions, under isothermal conditions, small molecules exhibit larger diffusivities since their v^* values are smaller relative to those of polymers. Therefore, v^* is the characteristic of diffusing molecules and $v_{free,\ average}$ is related to the properties of diffusing molecules and polymeric matrices. Practically, the physical stability of drug-polymer dispersions is highly correlated with the diffusivity of a drug molecule in a polymeric matrix; hence the selection of an appropriate polymer is very critical. To study the impact of drug mobility, Vogel-Tamman-Fulcher (VTF) equation, derived based on the free volume concept, has been used to predict the physical instability of drug-polymer dispersions under accelerated conditions [22].

Although the concept of free volume is commonly used to interpret the behavior of glass transition and to predict the temperature dependence of relaxation time-through VTF equation, a rigorous thermodynamic analysis was not available until Simha and Somcynsky (SS) published their paper in 1969 [23]. Based on Prigogine's arguments about the equation of state for mixing of polymers, Simha and Somcynsky derived an expression for the free volume of polymers in amorphous phases employing the combinatorial technique used by Flory and Huggins, and the detail will be presented later [23, 24]. The theory by Simha and Somcynsky provides a theoretical foundation to calculate the fractional free volume of amorphous phases, and its prediction is in general consistent with the results from pressure volume temperature (PVT) experiments [25]. Despite the utility of the fractional free volume from PVT results through SS analysis, a practical technique to measure free volume was not available until the appearance of positron annihilation lifetime spectroscopy (PALS) [26]. In the last decade, the development of PALS has provided a simple technique to measure the free volume (hole-size) of polymeric systems [27]. In addition, PALS also can provide structural information about the material tested [28]. The details of PALS measurement and analysis will be discussed later.

In this study, two poorly water-soluble drugs (IMC and ketoconazole-Keto) and four polymers (PVP, PVPA, HPC, and HPMCAS) have been chosen to prepare drug-polymer

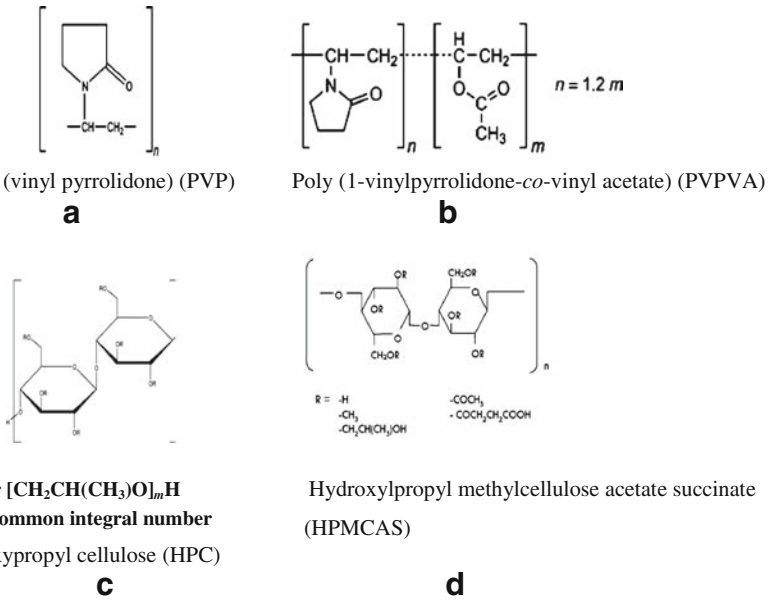

Fig. 1 The chemical structures of PVP (**a**), PVPVA (**b**), HPC (**c**), and HPMCAS (**d**).

dispersions through spray drying, which will be referred to as dispersions or spray dried dispersions (SDDs) in the rest of text. The appearance of SDDs was examined using scanning electron microscopy (SEM), and their amorphous nature was confirmed based on the results from powder X-ray diffraction (PXRD). The free volume of APIs, polymers, and SDDs was evaluated; hole-size was measured using PALS; in addition the fractional free volume of four polymers was obtained based on PVT results *via* SS analysis. Furthermore, the glass transition temperatures (Tgs) of SDDs along with their individual components were determined by differential scanning calorimetry (DSC). From the results of free volume and Tg, the effect of the polymer chain flexibility on the mixing behavior of free volume and glass transition was investigated. Furthermore, molecular interactions such as hydrogen bonding between polymer and API were assessed using Fourier transform infrared spectroscopy (FTIR) to address deviations from ideality. Finally, the polymer chain inflexibility as well as the hydrogen bonding interaction between drugs and polymers will be used to interpret the negative deviation of free volume from ideal mixing as well as the negative deviation in Tg from the predictions of Gordon-Taylor (G-T) calculation.

MATERIALS AND METHODS

Materials

PVP K29/32 (M_w=44,000-54,000 Da) was obtained from Ashland Chemicals Inc. (Wayne, NJ, USA), and PVPVA (VA64) was purchased from BASF Chemical Company (Florham Park, NJ, USA). HPC (L grade, M_w=140,000 Da) was acquired from Nisso America Inc. (New York, NY, USA), and HPMCAS (MG grade, M_w=18,000 Da; 9% acetyl and 11% Succinoyl) was a gift from Shin Etsu Chemical Co. (New York, NY, USA). Two poorly water-soluble drugs (IMC and Keto), purchased from Sigma-Aldrich Corp. (St. Louis, MO, USA) and Spectrum Chemical Manufacturing Corp. (Gardena, CA, USA) respectively, were used as model compounds. Processing solvents, acetone and methanol, were obtained from Sigma-Aldrich Corp (St. Louis, MO, USA).

Sample Preparation

Preparation of Spray Dried Dispersion

In general, SDD samples were prepared by dissolving drug-polymer pairs in their corresponding solvent/solvents followed by spray drying. For most of SDD samples, an API to polymer ratio of 25:100 was used based on the current practice in the pharmaceutical industry for preparing SDD using HPMCAS. In the case of IMC-HPMCAS dispersions, other ratios were also employed to explore the concentration effect of the polymer. For preparing IMC-HPMCAS dispersions, 3.3% (w/v) IMC-HPMCAS solution in acetone was first made by dissolving 10 g of the drug-polymer mixture in acetone with a total volume of 300 mL. The ratio of IMC to HPMCAS (w/w) was varied from 10%, 25%, and 35% to 45%. These solutions were then dried using a Buchi model B-290 laboratory spray drier (Buchi Corporation, New Castle, DE, USA). Spray drying conditions included aspiration (73%), pump rate (8%), nozzle cleaning-5, and inlet temperature (60–63°C). The same solvent and drying conditions were used to prepare the dispersions of IMC-HPC at 25% (w/w) IMC concentration. To prepare the dispersions of IMC-PVP and IMC-PVPVA at 25% (w/w) IMC

concentration, methanol was used as a solvent. Since methanol has a higher boiling point, the inlet temperature was kept at 70–73°C with other drying conditions remained the same.

Because ketoconazole has limited solubility in acetone, a mixed solvent of acetone and methanol (50:50, v/v) was used in preparing the dispersions of Keto-HPMCAS and Keto-HPC at 25% (w/w) Keto concentration. In this case, an inlet temperature of 70–73°C was used because of the high boiling point of methanol. Similarly, the dispersions of Keto-PVP (25%, w/w) and Keto-PVPVA (25%, w/w) were also prepared using methanol solvent with the same drying conditions.

Similar to SDDs, spray dried samples of polymers were prepared by dissolving polymers in either acetone (HPC and HPMCAS) or methanol (PVP and PVPVA) followed by drying at 60–63°C and 70–73°C of inlet temperatures. Likewise, the amorphous samples of IMC and Keto were prepared using either acetone or methanol with its corresponding drying conditions, respectively. Finally, for all preparations, the flow rate of inert gas-nitrogen was kept at 40 mL. Prior to any measurements, all SDD samples were vacuum-dried overnight at ambient temperature to ensure that residual solvent was completely removed.

Preparation of Film Samples

The film samples of PVP, PVPVA, HPC, and HPMCAS were prepared by casting 5-10% (w/w) of solutions of these polymers in their respective solvents: (1) PVP K29/23 and PVPVA in methanol, and (2) HPMCAS and HPC in acetone. Teflon and Teflon-coated Petri dishes were used for film casting, and the polymer solutions were dried overnight in a fume hood. All film samples were further dried overnight in a vacuum-oven at ambient temperature to remove the residual solvent.

PALS Measurement

The SDD samples for PALS measurement were prepared by pressing the powders of each SDD into a pellet of 1–2 mm in thickness and 10 mm in diameter using a Carver Press (Model 3888-1D10A00, Carver Inc. Wabash, IN, USA). Typically, 50–150 mg sample was transferred into a die of 10 mm in diameter followed by pressing using a force of 1,500 lb with 50% pump speed followed by 15 s dwelling. Film samples for PALS measurement were prepared by cutting polymer films into 10 mm in diameter and stacking up to 2 mm in thickness. To perform PALS measurement, about 1 MBq of ^{22}NaCl was deposited in an envelope of aluminum foil (1.7 mg/cm) and then sandwiched between two sample disks, held together with a non-adhesive Teflon tape. After, the sample assembly with ^{22}Na was placed in the sample chamber between photomultiplier tubes (PMTs). PALS experiments were conducted with a fast-fast coincidence system. In terms of measuring principle, the positrons emitted by the ^{22}Na nuclei are annihilated in a sample, producing 0.511 MeV γ-rays which signal annihilation. The positron's lifetime is measurable because the daughter nucleus, ^{22}Ne, also emits a 1.275 MeV γ-rays within 3 ps of the positron creation. The time difference between 1.27 MeV quanta and 0.511 MeV quanta (annihilation process) is the positron life time. Experimentally, the temperature for the sample in a vacuum chamber was controlled by heating wires to be about. 20±0.2°C. All spectra were collected on a PCA multichannel analyzer and a typical measurement took about 1 h with 1×10^6 counts for typical PALS spectrum. All PALS spectra were analyzed using PATFIT-88 software.

Pressure Volume Temperature Measurement (PVT)

In principle, PVT measures the change in specific volume as a function of temperature and pressure. The sample used in PVT measurements typically has volume of about 1 cm^3. To conduct a PVT experiment, a polymer film, with known volume (about 1 cm^3) and mass, was loaded in a rigid sample cell with calibrated volume. The remaining volume was filled with mercury. As a part of this rigid sample chamber, a flexible bellows was attached to a linear variable differential transformer (LVDT) sensor which allowed the sample to expand under an applied stimulus of heat or pressure. This LVDT read out allowed for the detection of small changes in volume. To start an experiment, hydraulic oil pump was used to pressurize the rigid cell and bellows by applying pressure directly to the confining fluid and the polymer sample through the bellow. Temperature was controlled using a heat chamber. In general, tests conducted include isothermal and isobaric measurements. For isothermal tests, the pressure of the sample was increased while retaining a constant temperature where adiabatic heating was conventionally considered minimal. To complete the isothermal tests, a range of temperatures were probed in one testing series. For isobaric tests, the pressure of the sample cell was retained while increasing or decreasing the temperature of the cell. Again, multi-pressure values were probed during isobaric experiments. Above testing protocol yielded high resolution Vs-P-T plots. The typical testing temperature ranged from 30°C to 400°C and the typical testing pressure ranged from10 MPa to 200 MPa. Based on the Vs (specific volume)-P-T plots generated from PVT data, occupied volume (V_{occ}) and thus the fractional free volume can be determined through melt state analysis using Simha-Somcynsky equations of state (SS-EOS) [29].

Glass Transition Temperature Measurement

Differential Scanning Calorimetry (DSC)

A TA Instruments Q1000 DSC (New Castle, DE, USA), calibrated using indium and maintained by TA, was used to

analyze all polymer, API, and SDD samples. Typically, 5–10 mg of each sample was weighed out and transferred into an aluminum DSC pan. Then, the pan was immediately crimped and transferred onto a DSC carousel. To acquire DSC thermograms, the following scanning parameters were used. After equilibration at 25°C for 5 min, modulated DSC experiments were performed with a modulation rate of 0.5°C per minute and scanning rate of 2°C per minute. For all samples, the scanning range was from 25°C to 175°C. For all experiments, nitrogen was used as the purge gas and the typical flow rate was 50 mL per min. To determine Tg, all thermograms were analyzed using the TA Universal Analysis Software, and individually, the temperature from the inflection point was taken as the Tg value, where the measured value was within the range of ±2°C in comparison with the ones reported in literature.

Dynamic Mechanical Analysis (DMA)

A TA Instruments Q800 DMA with a powder fixture in a powder clamp (TA instrument, New Castle, DE, USA) was used to analyze the HPC and HPC based dispersions. To start, a sample was first transferred to a sample holder followed by increasing temperature from room temperature to 150°C at 3°C per min with 1 Hz oscillation and 10 μm amplitude, where the storage and loss modulus, as well as the phase angle, tan δ, were displayed as a function of temperature.

Powder X-ray Diffraction (PXRD)

PXRD patterns were recorded on a Bruker D4 Endeavor/Lynxeye (Bruker, Germany) X-ray powder diffractometer with Cu Kα radiation: λ=1.541 Å. The diffractometer was equipped with a ceramic tube, which was set at the power level of 40 kV and 40 mA, and a PSD Lynxeye detector. Incident optics consisted of a 0.6° divergence slit. Diffracted optics consisted of Ni-K-Beta filter and the detector with a window of 3°. Data were collected in reflectance geometry, without spinning, over a 2θ range of 4–32°, where a step size of 0.03° and counting time of 1 s/step in continuous mode were employed.

Scanning Electron Microscopy

A scanning electron microscope (SEM) Lab6 XL-30 ESEM from FEI (FEI Electron Optics, Eindhoven, the Netherlands) was used to acquire images of the SDDs in a high vacuum using a secondary electron detector. Placed on a Carbon tab on aluminum stub, all samples were sputter-coated using a Cressington 208 h High Resolution Sputter Coater equipped with a platinum target (Ted Pella, Inc., Redding, CA).

Infrared Spectroscopy Measurement

The IR spectra were collected using a FTIR-ATR spectrometer (Nicolet NEXUS 670, ThermoFisher Scientific, Madison, WI, USA). Each spectrum was measured by accumulating 64 scans at 4 cm^{-1} spectral resolution over the range from 500 cm^{-1} to 4,000 cm^{-1} at ambient temperature.

RESULTS

As depicted in Fig. 2, the morphological appearance of SDDs (Keto-HPMCAS (a), IMC-PVP (b), IMC-HPMCAS (c), and Keto-PVP (d)) appears to be spherical or close to spherical, typical shapes of spray dried materials, although, in comparison, the SDD particles of Keto-PVP seems more spherical and smaller. Similar morphological shape was observed for the SDD particles of other drug-polymer pairs (data not shown here). To confirm the amorphous nature of SDDs, Fig. 3 displays the overlay of a few selected PXRD patterns of SDDs (pattern a) (25%, w/w) of drug-polymer pairs: IMC-HPMCAS, IMC-PVP, Keto-HPMCAS, and Keto-PVP along with their corresponding polymers (pattern b) and that of crystalline drugs (pattern c). As demonstrated in Fig. 3, the SDDs of IMC and Keto with either HPMCAS or PVP were all amorphous with a similar pattern to that of the polymer used. In addition, the SDDs of these drugs prepared with HPC and PVPVA as well as the SDDs of IMC-HPMCAS at other concentrations were all confirmed to be amorphous by PXRD (data not shown here).

Free volume

Since PALS measures the molecular or atomic interstitial volume, fundamentally, the hole-size obtained from PALS is independent of sample form, whether powder compact or polymer film as long as it is produced from the same solvent. This assumption is supported by comparing the hole-size results measured for HPMCAS film (85.3±2.8 $Å^3$) and powder compact (87.6±6.5 $Å^3$).

Fractional Free Volume from PVT

Figure 4 shows the fractional free volume of four polymers as a function of temperature. Evidently, the fractional free volumes of HPC and HPMCAS (cellulose derivatives) are larger relative to those of PVP and PVPVA (polyvinyl). In addition, within each group, the free volume of HPC is bigger than that of HPMCAS, and the free volume of PVPVA is larger in comparison with that of PVP. Overall, the following ranking order was observed: HPC > HPMCAS > PVPVA > PVP. Furthermore, as shown in Fig. 4, the fractional free volume

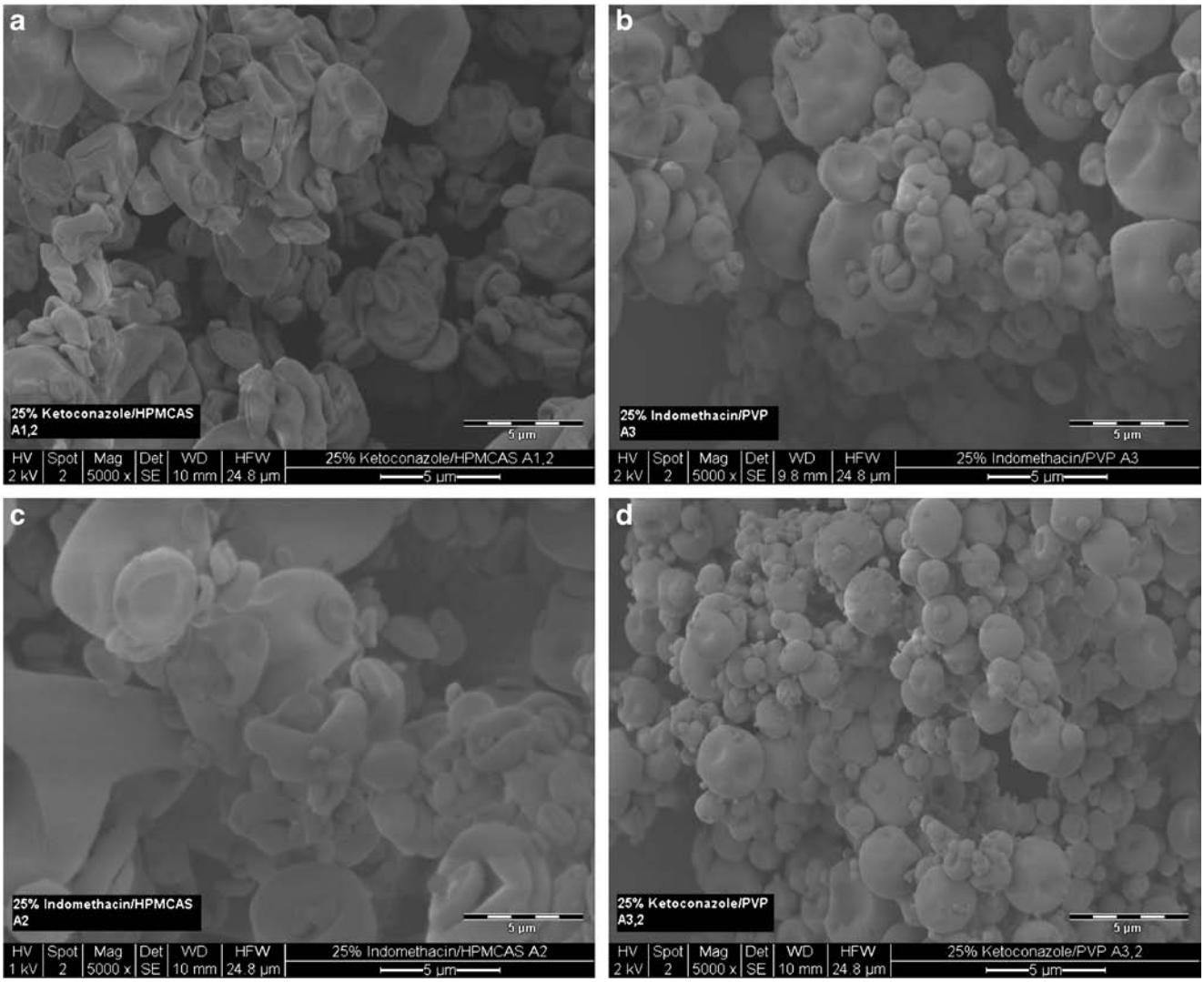

Fig. 2 SEM monographs of SDDs (25% drug concentration, w/w) of IMC and Keto with PVP and HPMCAS: Keto-HPMCAS (*top left-a*); IMC-PVP (*top right-b*); IMC-HPMCAS (*bottom left-c*); Keto-PVP (*bottom right-d*).

increased with temperature for all polymers, and inflection points (glass transition) were observed for three polymers except for HPC, which is due to its thermal insensitivity. These results, although different, are in general supportive of the results obtained with PALS.

Free Volume by PALS

Table 1 shows the average values of hole-size of IMC, Keto, PVP, PVPVA, HPMCAS, and HPC, where the hole-size of IMC and Keto (small organic molecules) is smaller compared with that of PVP, PVPVA, HPMCAS, and HPC (polymeric material). This observation is consistent with that reported in literature because small molecules can be easily compacted whereas the movement of polymeric molecules in solution is restricted by their chain connectivity [30–32]. Comparing cellulose derivatives with polyvinyl based polymers, HPMCAS and HPC have larger holes compared with PVP. This can be explained by the fact that the chains of PVP in solution are flexible so that they can fold on themselves and form tighter clusters in solution; In contrast, HPMCAS and HPC have rigid chains and their motion in solution is severely restricted by their backbone [33]. Regarding PVPVA, it is suspected that its solution behavior is dominated by its hydrophobic characteristics [34]. Furthermore, when polymers were mixed with small molecules, such as IMC or Keto, to form amorphous dispersions, the hole-size (free volume) of the dispersions was reduced (Table 2). Table 2 shows the average values of hole-size of SDDs of drug-polymer pairs, where the values of hole-size of SDDs lies between those of drugs (IMC and Keto), and those of polymers (PVP, PVPVA, HPC and HPMCAS). This is expected as reported on polymer blends in literature, suggesting that the empty spaces (holes) of polymers in SDDs were probably filled out with small molecules, and

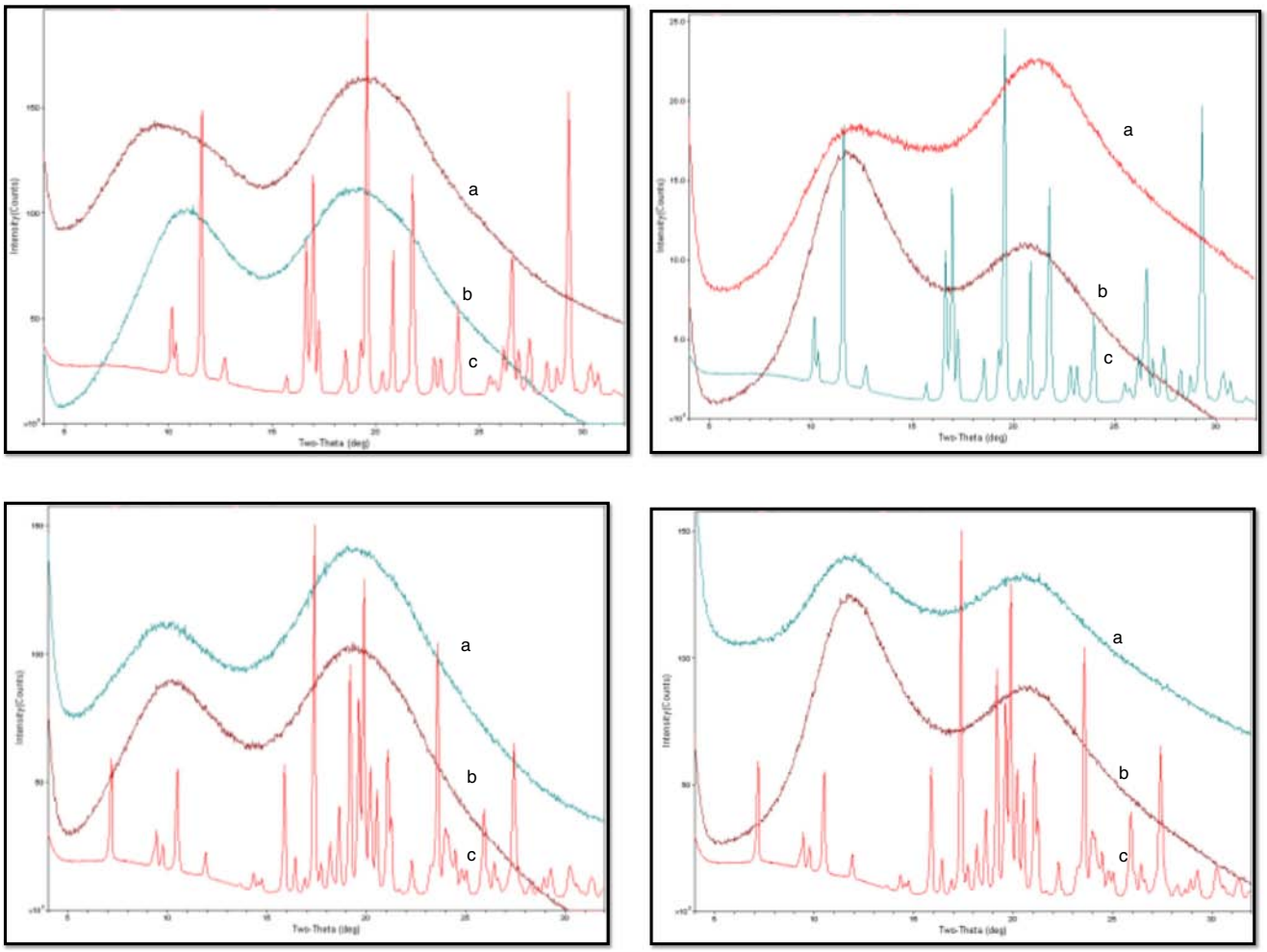

Fig. 3 PXRD patterns of IMC, Keto, HPMCAS, PVP, and their corresponding SDDs at 25% drug concentration (w/w): top left-IMC(**c**), HPMCAS (**b**), and IMC-HPMCAS dispersion (**a**); top right- IMC (**c**), PVP (**b**), and IMC-PVP dispersion (**a**); bottom left-Keto (**c**), HPMCAS (**b**), and Keto-HPMCAS dispersion (**a**); bottom right-Keto (**c**), PVP (**b**), and Keto-PVP dispersion (**a**).

thus the average size of holes in a SDD decreased due to mixing of small molecules with polymeric molecules [35]. To further study this, the average values of hole-size for the dispersions of IMC-HPMCAS with IMC concentration varied from 10% (w/w) to 45% (w/w) were measured (see Table 3). As indicated by Table 3, In general, the hole-size decreases with increasing IMC concentration, suggesting that with increasing the weight fraction of IMC, the holes between HPMCAS molecules or even within a HPMCAS molecule were filled out. This reduction of free volume relative to polymers or increase of free volume with regard to drugs in SDDs will inevitably impact the molecular mobility of SDDs

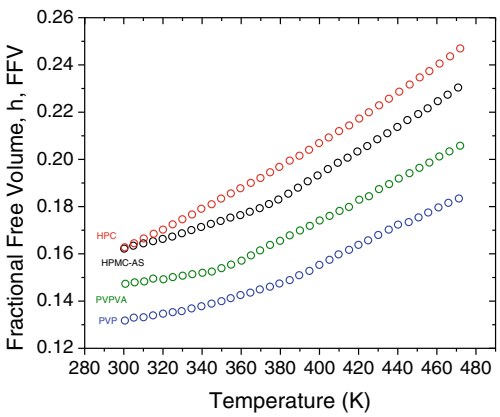

Fig. 4 Fractional free volume of four polymers obtained from PVT experiments (*from bottom to top*): PVP, PVPVA, HPMCAS, and HPC.

Table 1 The Average Values of Measured Hole-size of IMC, Keto, and Four Polymers-PVP, PVPVA, HPC, and HPMCAS

Sample	Measured hole-size volume ($Å^3$)
Indomethacin	42.0 ± 2.8
Ketoconazole	44.7 ± 2.6
PVP K29/32	64.1 ± 1.8
PVPVA	89.4 ± 1.8
HPC	89.2 ± 1.8
HPMCAS	87.6 ± 6.5

Table 2 The Average Values of Measured Hole-Size of SDDs at 25% (w/w) Drug Concentration as well as the Calculated Hole-Size Based on Volume Additivity (Eq. 8)

Sample	Measured hole-size volume (Å^3)	Calculated hole-size volume (Å^3)
25% Indomethacin/PVP	52.0 ± 2.3	58.6
25% Indomethacin/PVPVA	78.1 ± 2.4	77.6
25%Indomethacin/HPC	75.6 ± 2.4	77.4
25%Indomethacin/75%HPMCAS	73.6 ± 2.9	76.2
25%Ketoconazole/PVP	60.1 ± 2.1	59.3
25% Ketoconazole/PVPVA	76.9 ± 4.3	78.2
25%Ketoconazole/HPC	70.1 ± 2.7	78.1
25%Ketoconazole/HPMCAS	74 ± 2.7	76.9

which should be reflected in the glass transition behavior of SDDs.

Glass Transition Behavior

The glass transition behavior of SDDs was primarily investigated by measuring their Tg using DSC along with examining each individual thermogram. Since HPC exhibits a weak thermal signal in DSC, both DSC and DMA were used for Tg determination of HPC and the SDDs of HPC, where they are in general consistent except that Tg of HPC from DMA is higher relative to that by DSC due to the nature of measurement. However, because most of samples (Tg) were measured using DSC, Tg of HPC obtained from DSC was used in calculation. In Table 4, the Tg values of IMC, Keto, and four polymers are listed. In addition, as shown in Table 4, the predicted Tg values for SDDs of IMC and Keto with each polymer at a drug concentration of 25% (w/w), calculated based on G-T equation (Eq. 2), are listed to compare with the experimental values.

$$T_g = \frac{\left(w_1 T_{g1} + k w_2 T_{g2}\right)}{w_1 + k w_2} \quad (2)$$

where T_{g1} and T_{g2} are the glass transition temperatures of components 1 and 2; w_1 and w_2 are the weight fractions of components 1 and 2; K is the G-T correction factor, and it can be calculated based on the glass transition temperatures and density values of components 1 and 2 ($k=T_{g1}\rho_1/T_{g2}\rho_2$). In this paper, the following density values (g/mL): IMC (1.31), Keto (1.30), PVP (1.20), PVPVA (1.18), HPC (1.22), and HPMCAS (1.30) (from the manufacturer) were used in calculation [6, 11, 36].

As indicated in Table 4, the measured Tg values of IMC, Keto, and individual polymers are consistent with those reported in literatures (5, 11, 36,). Furthermore, for all SDDs, their experimental Tg values are lower than those calculated based on G-T equation (Eq.2), suggesting a negative deviation. Relative to the dispersions made with PVP and PVPVA, it appears that the SDDs prepared with HPMCAS and HPC showed a higher degree of negative deviation in Tg except for the SDD of Keto-HPMCAS. The possible reasons for this observation are: (1) hydrogen bonding interaction between drugs and polymers, (2) steric interactions, and (3) the effect of cellulosic structure-rigid backbone. To further confirm this, Tgs of the SDDs of IMC-HPMCAS with various concentrations of IMC (weight fraction) were determined (Table 5). Table 5 shows that as expected, the Tgs of IMC-HPMCAS dispersions decrease with increasing the weight fraction of IMC. In addition, the deviation of Tgs from their predicted values increase with the concentration of IMC, suggesting that the negative deviation in Tg can be due to either interactions (hydrogen bonding or steric) or the effect of the concentration of HPMCAS in SDDs. To confirm the presence of hydrogen-bonding interactions in these systems, the infrared spectra of the SDDs (25% w/w) were recorded. In addition, the infrared spectra of IMC, Keto, and individual polymers were also recorded for comparison.

Table 3 Average Values of Measured Hole-Size of IMC and HPMCAS, and SDDs at Various IMC Concentration as Well as the Calculated Values Based on Volume Additivity (Eq. 8)

Sample	Measured hole-size volume (Å^3)	Calculated hole-size volume (Å^3)
Indomethacin	42.0 ± 2.8	n/a
HPMCAS	87.6 ± 6.5	n/a
10% Indomethacin/90% HPMCAS	85.9 ± 1.8	83.4
25%Indomethacin/75%HPMCAS	73.6 ± 2.9	76.2
35%Indomethacin/65%HPMCAS	69.9 ± 1.7	71.6
45%Indomethacin/55%HPMCAS	65. ±2.10	67.1

Table 4 Glass Transition Temperatures, Measured by DSC and DMA, of API (IMC and Keto) and Polymers (PVP, PVPVA, HPC, and HPMCAS), as well as SDDs at 25% API Concentration (w/w)

Composition	Measured Tg (°C)	*Calculated Tg (°C)
HPC	100 (108.8)	n/a
PVP	173	n/a
PVPVA	108	n/a
HPMCAS	119	n/a
IMC	46	n/a
Keto	47	n/a
25% IMC/75%HPC	61 (51–62)	86
25% IMC/75%PVP	122	135
25% IMC/75% PVPVA	87	92
25% IMC/75% HPMCAS	69	98
25% Keto/75%HPC	53 (49.1)	86
25% Keto/75%PVP	124	135
25% Keto/75% PVPVA	88	92
25% Keto/75%HPMCAS	90	98

*G-T equation was used for glass transition temperature calculation, and the Tg vlaues reported in parenthesis were derived from TMA measurement. A standard deviation of ±2°C is in general applied to all DSC measurements. n/a denotes not applicable

Infrared Spectroscopy

Figure 5 shows the FTIR spectra of SDDs along with individual drugs and polymers. For the SDDs of IMC-PVP (Fig. 5a), the IR spectra indicated that the asymmetric stretch (1,708 cm^{-1}) of the carboxylic acid in a dimer structure significantly decreased in intensity as compared with that of IMC alone. In addition, a significant shift of the C=O peak, from 1,735 cm^{-1} (amorphous IMC) to 1,723 cm^{-1} (the SDD of IMC-PVP), was observed. This can be attributed to the formation of hydrogen bonding between the carboxylic acid group of IMC and the carbonyl group of PVP. Figure 5b shows the spectrum of the SDD of IMC-PVPVA, where the final spectrum was obtained by subtracting the spectrum of PVPVA from that of IMC-PVPVA. Similarly, the C=O peak of IMC at 1,736 cm^{-1} was found to shift to 1,725 cm^{-1} when it was dispersed within PVPVA, which is likely due to the formation of the hydrogen bonding between IMC and the PVP portion of PVPVA. Furthermore, a slight shift of benzoyl C=O at 1,678 cm^{-1} to 1,673 cm^{-1} was also observed in Fig. 5b. When the SDD of IMC with HPC was analyzed (Fig. 5c), the disappearance of the peaks at 1,736 cm^{-1} and 1,708 cm^{-1} along with the appearance of a new peak at 1,725 cm^{-1} were noted. In addition, no shifting of benzoyl C=O at 1,678 cm^{-1} toward lower wavenumber was seen. Examination of carbonyl region of the IR spectrum in the SDD of IMC with HMPCAS shows the presence of the same wavenumbers as for the pure components. In summary, IR data confirms the presence of the hydrogen bonding interaction between IMC and three polymers. The significant changes in IR spectra suggest that the strong hydrogen bonding interaction between IMC and PVP and PVPVA, and the moderate interaction between IMC and HPC, but less interaction for HPMCAS appears in solid dispersion as shown in Figs. 5a, b, c, and d.

For the SDDs of Keto with polymers, the IR spectra, shown in Figs. 4e and f, don't indicate any change of the C=O peak at 1,640 cm^{-1} for the Keto-PVP and Keto-PVPVA dispersions. In comparison, as shown in Figs. 5g and h, a significant shift of C=O peak towards a low wavenumber (1,628 cm^{-1} for Ketoconazole-HPC and 1,610 cm^{-1} in Keto-HPMCAS) was observed as shown, suggesting the formation of hydrogen bonding between the C=O group in Keto and -OH in HPC and HPMCAS. Overall, it appears that Keto interacts more with cellulosic derivatives as compared with PVP/PVPVA polymers.

Table 5 Glass Transition Temperatures Measured by DSC for IMC, HPMCAS, as well as SDDs of IMC-HPMCAS with Various IMC Concentrations

Composition	Measured Tg (°C)	*Calculated Tg (°C)
IMC	46	n/a
HPMCAS	119	n/a
10% IMC/90%HPMCAS	99	111
25% IMC/75%HPMCAS	69	98
35% IMC/65%HPMCAS	56	90
45% IMC/55% HPMCAS	54	83

*G-T equation was used for glass transition temperature calculation, and a standard deviation of ±2°C is in general applied to all measurements. n/a denotes not applicable

DISCUSSION

In this paper, we focus on the effect of flexible (polyvinyl molecules) and rigid (cellulose derivatives) chains on the free volume and glass transition temperatures of SDDs. Two polyvinyl polymers (PVP and PVPVA) and two cellulose derivatives (HPC and HPMCAS) were chosen for this study. In addition, two model drugs, both poorly water-soluble, were selected to prepare ASDs. Comparing indomethacin with ketocanozole, the former is readily to be crystallized alone while the latter remains stable at amorphous state although their Tg values are similar [37–39]. In the following section, a theoretical background on the solution behavior of flexible and rigid chain polymers is provided; in addition, the background on the techniques of measuring free volume (PALS for hole-size) and fractional free volume (PVT) will be briefly discussed.

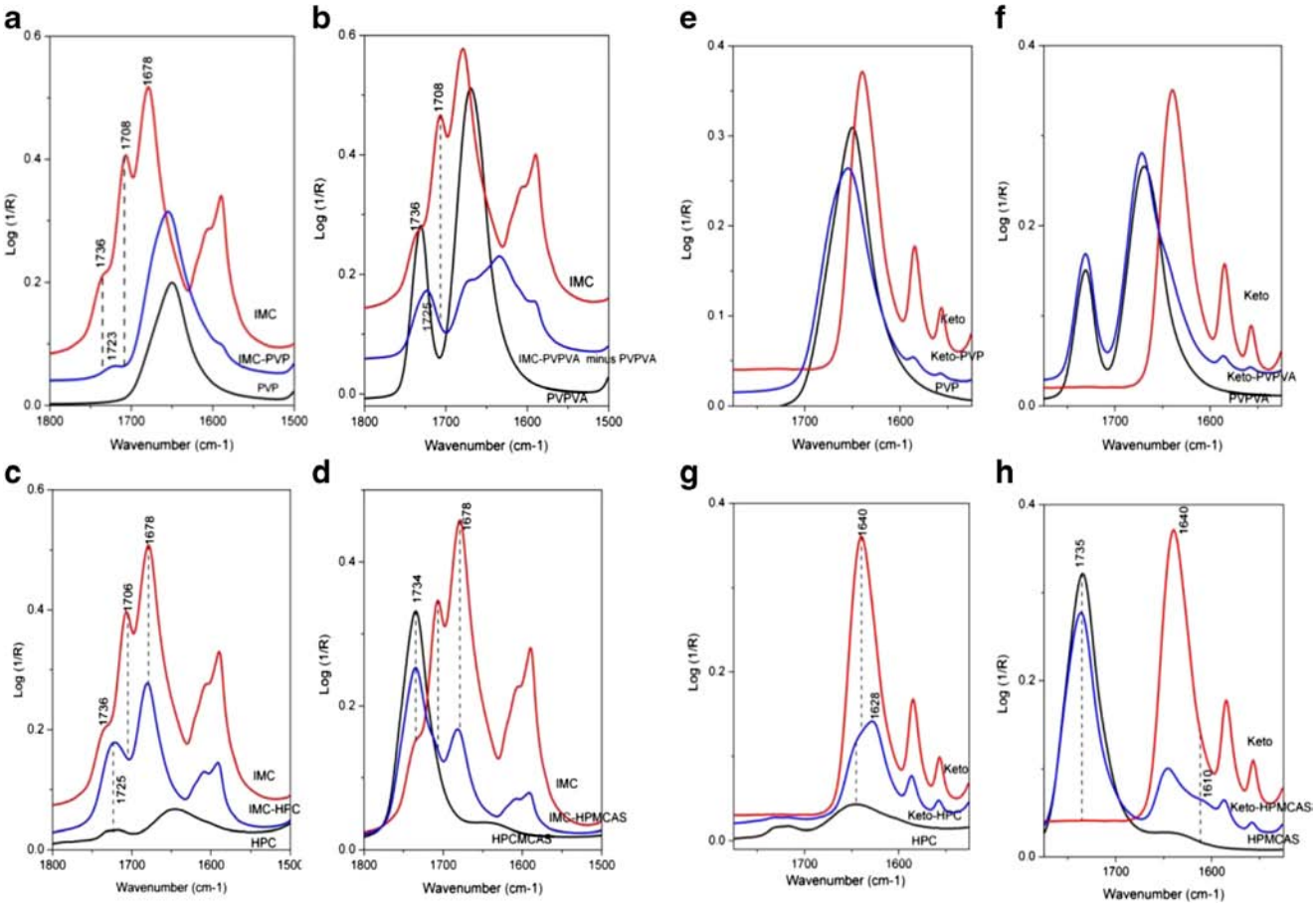

Fig. 5 FTIR spectra of SDDs along with drugs and polymers (*from bottom to top*): **a** PVP, IMC-PVP dispersion, and IMC; **b** PVPVA, IMC-PVPVA dispersion minus PVPVA, and IMC; **c** HPC, IMC-HPC dispersion, and IMC; **d** HPMCAS, IMC-HPMCAS dispersion, and IMC; **e** PVP, Keto- PVP dispersion, and Keto; **f** PVPVA, Keto-PVPVA dispersion, and Keto; **g** HPC, Keto-HPC dispersion, and Keto; **h** HPMCAS, Keto-HPMCAS dispersion, and Keto.

Theoretical Background

Conformational Dimensions of Polymers in Solution

As shown in Fig. 1, PVP (a) and PVPVA (b) are polyvinyl type of polymers with -C-C- backbone whereas HPC (c) and HPMCAS (d) are cellulose derivatives with D-glucopyranose in their backbone (β1-4 linkage). PVP and PVPVA are flexible because of their flexible carbon-carbon backbone structure (−C-C-); however, HPC and HPMCAS are inflexible or semi-flexible because the glucopyranosic structure at the backbone renders the glycosidic linkage inflexible (a typical angle of 112.5 °). For flexible chain polymers, random walk statistics has been used to model the conformations of polymers in solution, and, as a result, Gaussian distribution of chain is obtained. For flexible chains, the size of chain in solution is expressed as a radius of gyration (see Eq. 3).

$$R_g^2 = \frac{nl^2}{6} = \langle R^2 \rangle / 6 \tag{3}$$

where n, l, and $<R^2>$ are the number of segments, segment length, and mean square distance [17, 40].

For semi-flexible or inflexible chains such as cellulose derivatives (HPC and HPMCAS), the random walk model is inadequate to describe their behavior since their chains are not flexible. Therefore, a worm-like chain model was proposed by Kratky and Porod (KP model) for rigid chain molecules [17, 40]. The typical parameters used in this model are persistence length, q, and contour length, L, defined as:

$$\mathrm{L} = \lim_{N\to\infty} Na \quad \text{and} \quad q = \lim_{a\to 0\ \varphi\to 0} \frac{a}{1-\cos\varphi} \tag{4}$$

where N, a, and φ are the number of segments, segment length, and supplementary angle, respectively. Therefore, the mean-square end-to-end distance and the mean-square radius of gyration are:

$$\begin{aligned} \langle R^2 \rangle &= 2qL - 2q^2\left(1-e^{-\frac{L}{q}}\right) \text{ and } \left\langle R_g^2 \right\rangle \\ &= \left(\frac{qL}{3}\right) - q2 + \left(\frac{2q^3}{L}\right)\left\lfloor 1-\left(\frac{q}{L}\right)\left(1-e^{-\frac{L}{q}}\right)\right\rfloor \end{aligned} \tag{5}$$

When the rigidity of worm-like chains diminishes, (q is very small compared with L), they become Gaussian chains [17,

40]. As reported in the literature, the persistence length (3–25 nm) of cellulose derivatives are significantly larger compared with that of polyvinyl based polymers (about 1 nm) [41]. This conformational structure difference between polyvinyl polymer and cellulose derivative significantly impacts their molecular behavior, in particular their hydrodynamic behavior. As reported in the literature, the unperturbed chain dimension of cellulose derivatives is larger than that of polyvinyl polymers [18]. These properties are likely to be carried to the amorphous state after spray drying. Therefore, possibly, the structures of the SDDs made with cellulose derivatives are different from those made with polyvinyl based polymers. So, it is expected that the SDDs of cellulose derivatives such as HPC and HPMCAS would behave differently compared with the SDDs of PVP and PVPVA. As mentioned previously, even though PVPVA is a polyvinyl polymer, it is likely that the solution behavior of PVPVA is significantly altered by its hydrophobicity, and more research is needed in this area.

Free Volume by PVT and PALS Measurement

The thermodynamic foundation of free volume analysis for amorphous materials was laid based on SS theory [21, 23]. To develop the cell-hole theory for amorphous polymers, Simha and Somcynsky used a lattice-hole model, where the molecular segments of a s-mer were considered to occupy a y-fraction of lattice sites while the remaining sites (randomly distributed), h = 1-y, were treated as empty holes. The fraction, h, is a measure of the free-volume content. Simha and Somcynsky expressed the configurational partition function (Z) of the holes and the occupied sites in an amorphous state as a product of three factors as shown in Eq. 6: (1) a combinatory factor from mixing of y (occupied site) and h (free-volume) (g (N, y)), (2) a factor related to the external freedom of free volume $(V_f(V, y)^{CN})$, and (3) an exponential factor related to the potential of the system with all segments in the rest position.

$$\mathcal{Z} = g(\mathcal{N}, y)\left[v_f\ (V, y)\right]^{cN} \exp\left[-\frac{E_0\ (V, y)}{k_B T}\right] \tag{6}$$

The combinatory factor, g (N, y), was calculated using the Flory-Huggins method. The potential factor, exp $(-E_0(V, y)/k_BT)$, was calculated using the Lenard-Jones potential for E_0, and k_B and T are the Boltzmann constant and temperature. The free volume factor was expressed as $(V_f(V, y))^{CN}$ where V_f is the free volume and CN is the external freedom [23]. After linking Eq.6 to the Helmholtz free energy (F = −RTlnZ), F can be obtained. Then, the differentiation of F leads to SS equation at a thermodynamic equilibrium. Among all the equations of state, the SS equation of state is the only one with explicit expression of free volume (hole, 1-y). The SS results were further simplified by Simha and other authors, and resultant mathematical expression will be described in the Appendix.

PALS Analysis of Free Volume

Although the fractional free volume can be obtained from the results of PVT measurements *via* the analysis using SS equation, PALS provides another simple and non-destructive tool to evaluate the free volume in amorphous materials. As described in the experimental section, PALS measurement is based on the fact that when positrons from ^{22}Na are injected into the samples under investigation, some of them may form unstable electron-positron complexes (positronium-Ps). Ps can exist as ortho-Ps (parallel) (o-Ps) and para-Ps (antiparelle) (p-Ps), reflecting the different spin states of particles. In vacuum, o-Ps has life time of 142 ns while p-Ps only has a life time of 125 ps. In amorphous materials, o-Ps interacts with the electrons in the vicinity of the hole where it is trapped in; this process is termed annihilation or a pick-up mechanism, reducing the lifetime of o-Ps to about 1 to 10 ns. PALS measured the lifetime of o-Ps particles after their annihilation. The time measurement is based on the difference between the signal of birth of positron particles (1.274 MeV) and the annihilated positrons (0.511 MeV). The correlation between the annihilation decay rate and the size of the hole hosting Ps was suggested by Tao and further elaborated by Eldrup *et al.* [42, 43]. Their model assumed a spherical hole with an effective radius of R, and the hole, in which a Ps is trapped, has a potential well of finite depth which can be treated as infinite for the purpose of calculation. Based on this model, Eq. 7 has been derived.

$$\tau_3 = \frac{1}{\lambda_3} = \frac{1}{2}\left[1 - \frac{R}{R+\delta r} + \frac{1}{2\pi}\sin\left(\frac{2R}{R+\delta r}\right)\right]^{-1} \tag{7}$$

where τ_3 , λ_3 , R, and δr are the lifetime of positron after annihilation and decay rate, as well as the radius of the hole and the correction constant. The PALS spectra generally include the lifetime contribution of p-Ps, free positron and o-Ps. The de-convolution of these three contributions from a spectrum is usually performed using PATFIT-88 software that outputs the average life time and the relative fraction of positrons that annihilate from each of these Ps events. The resulting lifetimes (τ_1, τ_2, and τ_3) and intensities (I_1, I_2, and I_3) are reported. Since the first two Ps events occur at lifetimes much shorter than the long lived o-Ps, the data analysis focuses on the o-Ps lifetime and intensity, τ_3 and I_3. Eldrup and coworkers correlated τ_3 with void volumes in zeolite membranes with the assumption that the voids are spherical [43, 44]. The radius of a free volume element, R, is predicted

using a constant δr (0.1656 nm) and the experimentally determined τ_3. In this paper, all PALS spectra were analyzed as described above and the volume of hole-sizes was reported.

Free Volume of Amorphous Dispersions

As shown in Table 1, the average value of hole-size for IMC and Keto is around 42 $Å^3$, which is consistent with the value reported for small organic molecules [30]. However, the average value of hole-size for polymers is, in general, much larger in comparison (Table 1). Particularly, polymers of cellulose derivatives (HPMCAS and HPC) have larger holes relative to PVP. Since the amorphous state is regarded as super-cooled liquids, their structures in liquid state are possibly maintained after solidification. Specifically, because the conformations of PVP (a polyvinyl polymer) in solution are Gaussian-like with persistence length about 1 nm-very compacted, the hole-size of PVP polymer is smaller as the compacted conformations are likely being retained after drying. In comparison, cellulose derivatives are known to be inflexible in solution due to their rigid chains, preventing the molecules from bending to form compact structures in solution (persistence length 3–25 nm). Therefore, it is possible that the loosen structures of HPMCAS and HPC in solution are partially carried to solid state after drying, causing their holess to be larger than that of PVP. Regarding PVPVA, since it is a copolymer with a hydrophobic side chain of vinyl acetate, it is likely that its chain can be stretched out and be expanded in a favorable solvent; as a result, the hole-size of the spray dried PVPVA is much larger than that of PVP. This observation needs to be further investigated with other copolymers. When mixing either IMC or Keto with a polymer to form a binary dispersion such as a SDD in this paper, it is expected that the free volume of the SDD will be somewhere in between that of the polymer and that of the small molecule due to blending at a molecular level. For ideal mixing, the free volume (hole-size) of the SDD is the sum of the free volume of two components based on the rule of additivity. However, due to the interactions between the API and the polymer as well as the non-ideality of mixing, deviation can occur as modeled by Eq. 8

$$V = V_1 w_1 + V_2 w_2 + k w_1 w_2 V_1 V_2 \tag{8}$$

where V, V_1, and V_2 represent the hole-size (volume) of SDD, components 1, and component 2; w_1, w_2, and k are the weight fraction of components 1 and 2, and interaction constant, respectively [35].

As shown in Table 2, compared with the predicted values using Eq. 8, the measured hole-size shows a significant deviation when strong interactions between drugs and polymers are involved. For IMC-PVP dispersion, it appears that due to the strong interaction between IMC and PVP, the measured hole-size (the actual free volume) shows a significant deviation relative to the calculated hole-size (predicted free volume based on ideal mixing). In comparison, for IMC-HPC and IMC-HPMCAS dispersions, the deviation is much less or none (with consideration of experimental error) since the hydrogen bonding interaction is much weaker in these systems as evidenced by the small shift of peaks in FTIR spectra. A different trend was observed for Keto-polymer dispersions. It seems that there is no deviation observed since Keto does not interact with PVP through hydrogen bonding. In contrast, a significant deviation in hole-size was noticed for the SDD of Keto-HPC, possibly because of strong hydrogen bonding. Again, for the SDD of Keto-HPMCAS, the deviation is much less, (almost negligible with experimental error) due to a weak hydrogen bonding interaction. To systematically investigate the free volume deviation in terms of hole-size for IMC-HPMCAS dispersions, both measured and calculated hole-size values are plotted as a function of IMC concentration as seen in Fig. 6a. Figure 6a clearly shows that the hole-size deviation in these dispersions is insignificant even though it seems that the deviation is largest at 25% (w/w) IMC concentration. Interestingly, at the IMC concentration of 10% (w/w), the dispersion displays a positive deviation in hole-size. Generally, the free volume change with temperature can be used to interpret glass transition, and therefore it would be interesting to compare the free volume deviation with the glass transition behavior of SDDs.

Glass Transition Temperature

Free volume always increases with temperature, and it reaches the iso-free volume (2.5%) at glass transition. As expected (Table 4), IMC and Keto-small organic molecules-have similar but lower Tgs relative to those of polymers, suggesting that they can expand quickly as temperature is raised. In comparison, PVP, PVPVA, HPC, and HPMCAS have higher Tgs, indicating a less volume expansion with temperature. For the Tg values of drug-polymer dispersions, as exhibited in Table 4, the experimental Tgs of all SDDs are lower than those predicted based on G-T equation, suggesting a negative deviation. In particular, it appears that a larger deviation in Tg was observed for IMC-HPC or IMC-HPMCAS dispersions (cellulose derivatives), compared with the dispersions of IMC-PVP or IMC-PVPVA. This observation is different from the trend of free volume deviation, where the dispersion of IMC-PVP showed the largest deviation due to hydrogen bonding interaction. As indicated in literature, the deviation of glass transition temperature can be due to interactions such as hydrogen bonding and other factors like steric interaction [45]. To incorporate these factors to predict Tg, Kwei and coworkers formulated an equation by adding an interaction term to the G-T equation (Eq. 9),

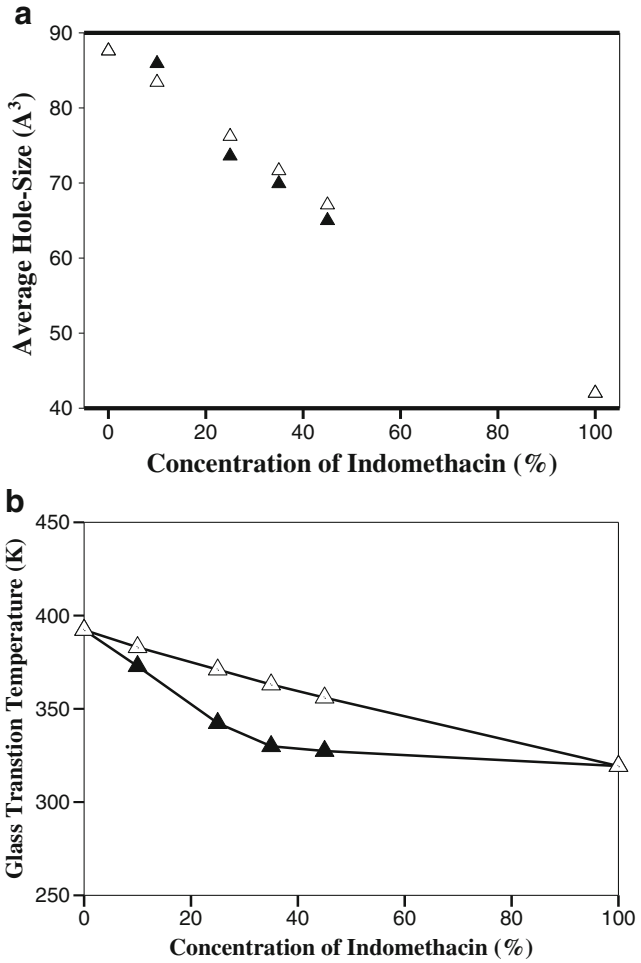

Fig. 6 **a** Average hole-size as a function of IMC concentration for IMC-HPMCAS dispersions: measured values (▲) and the calculated values based on Eq. 8 (Δ). **b** Glass transition temperatures of SDDs as a function of IMC concentration for IMC-HPMCAS dispersions: measured values (▲) and calculated values using G-T equation (Eq. 2) (Δ).

$$T_g = \frac{\left(w_1 T_{g1} + k w_2 T_{g2}\right)}{w_1 + k w_2} + q w_1 w_2 \qquad (9)$$

where T_g, T_{g1}, and T_{g2} are the Tgs of a dispersion, and components 1 and 2; w_1 and w_2 represent the weight fractions of components 1 and 2; k and q are the G-T correction factor and interaction constant, respectively [45]. As assumed, hydrogen bonding interaction would always increase Tg, and therefore, q should be always positive. However, it was found later that for many polymer-polymer blends, q can be negative, because of other factors such as steric interaction [45]. Similarly, for the SDDs reported in this paper, if hydrogen bonding were the only contributing factor to Tg deviation, it would be positive rather than negative. Therefore, there must be other factors involved such as steric interaction. In particular, comparing the Tgs of SDDs of PVP and PVPVA with the Tgs of SDDs of HPC and HPMCAS, a larger negative deviation is generally observed for the dispersions prepared with cellulose derivatives. The explanation for this observation can be two folds. First, although for the dispersions of both polyvinyl based polymers and cellulose derivatives, it is suspected that steric interaction will contribute to the negative deviation in Tg, possibly, the contribution of steric interaction in the dispersions of cellulose derivative is much larger owing to the rigid structure of their chains. Secondly, since G-T was developed for the flexible chain polymer system, the predicted Tgs for the dispersions with polymers of rigid chain may not be accurate [46, 47]. This can be illustrated by systematically investigating the Tg deviation of IMC-HPMCAS dispersions. As shown in Fig. 6b, for the SDDs of IMC-HPMCAS, the trend for Tg deviation (negative) appears to be larger compared with that of free volume (hole-size); in particular, the deviation reached a maximum at 50% IMC concentration (w/w). After all, relative to glass transition temperature, it appears that free volume correlates better with hydrogen bonding. In summary, the structural difference in terms of chain rigidity, between cellulose derivatives and polyvinyl polymers, are clearly reflected in the free volume and glass transition of SDDs prepared with these polymers. As regarding the dispersion of drug-PVPVA, the hydrophobicity of PVPVA will likely dominate their free volume behavior. This difference will potentially impact the performance of SDDs and ultimately influence the decision of polymer selection.

Selection of Excipients

The selection of an appropriate polymeric excipient is critical for preparing SDDs since polymers not only affect the physical stability of drugs but also impact their dissolution in the final dosage forms, ultimately influencing the bioavailability of the drugs. Currently, choosing a polymeric excipient for a SDD formulation is commonly based on historical success using that particular polymer for dosage form development. Prior to the acceptance of HPMCAS, PVP was the choice of polymer to prepare drug-polymer solid dispersions. Although PVP 32/29 has a high Tg (~170°C), its hydrophilic property often renders the dispersions of drug-PVP physically instable when being exposed to moisture. Since the introduction of HPMCAS, the number of SDD formulations with it has increased significantly. As shown in this paper, the physical properties of cellulose derivatives are significantly different from polyvinyl polymers due to the uniqueness of their chemical structures. In addition, all other attributes of polymers, such as Tg, hydrogen bonding, and interaction with water, should be considered when choosing a polymeric excipient. Finally, it appears that the unique properties of cellulose derivatives such as a large

free volume may influence the performance (stability and dissolution) of their SDDs which will be investigated later.

CONCLUSIONS

Based on the results in this paper, it can be concluded that free volume, as the hole-size measured using PALS, is a critical characteristic of amorphous phases, which should be evaluated for amorphous dispersions such as SDDs. In addition, due to their structural differences-particularly backbones (inflexible [HPC and HPMCAS] *vs.* flexible [PVP and PVPVA]), pharmaceutical polymeric excipients exhibit varied free volumes. This can also impact the free volume of amorphous dispersions prepared with these polymers. Furthermore, a negative deviation, in terms of free volume and Tg, from ideal mixing was generally observed for most of the SDDs. In fact, the deviation in hole-size displays a good correlation with hydrogen bonding interaction as detected by FTIR. In contrast, the deviation of Tgs from the prediction of G-T equation is less correlated with hydrogen bonding interaction. Reasons for the negative deviation of cellulose derivative in Tg are possibly due to a large contribution of steric interaction and the improperness of using G-T equation for systems involved rigid chains. Thus, free volume (hole-size) seems to yield a better prediction for specific interactions such as hydrogen bonding. Additionally, it appears that the free volume of amorphous phases of polymers or their SDDs is related to the conformational structures of polymers in solution; cellulose derivatives (inflexible chains) with larger unperturbed chain dimensions in solution also exhibit larger free volume after drying compared with PVP and the SDDs of PVP that its solution conformation is Gaussian-like. This is very important since it allows for connecting the properties of SDDs with the solution behaviors of these polymers. Overall, this paper demonstrated the utility of free volume (hole-size) as measured by PALS for understanding pharmaceutical materials as well as the effect of chain structure of these pharmaceutical relevant polymers, particularly cellulose derivative, on the free volume and glass transition temperatures of SDDs

ACKNOWLEDGEMENTS AND DISCLOSURES

Authors would like to thank the management of Drug Product Science & Technology at Bristol-Myers Squibb for financial support as well as Prof. Nazarenko and Mr. Goetz of the University of Southern Mississippi for providing free volume and fractional free volume results used in this paper and supplying the experimental procedure used. In addition, authors are grateful to Dr. Hussain of Bristol-Myers Squibb for reading the manuscript.

APPENDIX

Specific Volume and Fractional Free Volume from P-V-T [24, 26]

After simplification, the SS equation of state can be expressed as the following:

$$V(p,T) = V^* * exp\left(a_0 + a_1\left(\frac{T}{T^*}\right)^{\frac{3}{2}} + \left(\frac{p}{p^*}\right)\left[a_2 + \left(a_3 + a_4\left(\frac{p}{p^*}\right) + a_5\left(\frac{p}{p^*}\right)^2\right) * \left(\frac{T}{T^*}\right)^2\right]\right) \quad (1)$$

Where $a_0 = 0.0921$, $a_1 = 4.892$, T*, P*, and V* are the conditions at the material's critical point. The data shown is found using a Tate extrapolation to 0 MPa, allowing the reduction of the above equation to

$$\ln(V) = \ln(V^*) - a_0 + a_1 * T^{\frac{3}{2}} * \left(\frac{1}{T^*}\right)^{\frac{3}{2}} \quad (2)$$

Occupied volume, V_{occ}, was calculated using the following equation where y_{occ} is the occupied fraction, $\widetilde{P}$, $\widetilde{T}$, and $\widetilde{V}$ are reduced parameters:

$$\widetilde{P} = \frac{P}{P^*} \quad \widetilde{T} = \frac{T}{T^*} \quad \widetilde{V} = \frac{V}{V^*}$$

$$\frac{\widetilde{P}\,\widetilde{T}}{\widetilde{V}} = \left[1 - y * \left(2^{\frac{1}{2}} * y_{occ} * \widetilde{V}\right)^{\frac{1}{3}}\right]^{-1} + \frac{y_{occ}}{\widetilde{T}}\left[2.002 * \left(y_{occ} * \widetilde{V}\right)^{-4} - 2.409 * \left(y_{occ} * \widetilde{V}\right)^{-2}\right] \quad (3)$$

$$V_{occ} = V_{sp} * y_{occ} \quad (4)$$

Fractional free volume, FFV, can be calculated using:

$$FFV = 1 - y_{occ} \quad (5)$$

REFERENCES

1. Friesen DT, Shanker R, Crew M, Smithey DT, Curatolo WJ, Nightingale JAS. Hydroxypropyl methylcellulose acetate succinate-based spray-dried dispersions: an overview. Mol Pharm. 2008;5: 1003–19.
2. Yonemochi E. Estimation of physicochemical stability of the formulation using solid dispersion technique and its application for formulation design. Pharm Tech Jpn. 2010;26:661–6.
3. Laitine R, Lobmann K, Strachan CJ, Grohganz H, Rades T. Emerging trends in the stabilization of amorphous drugs. Int J Pharm. 2013;453:65–79.
4. Wegiel LA, Mauer LJ, Edgar KJ, Taylor LS. Crystallization of amorphous solid dispersions of resveratrol during preparation and storage-impact of different polymers. J Pharm Sci. 2013;102:171–84.
5. Paudel A, Humbeeck J, Van Den Mooter G. Theoretical and experimental investigation on the solid solubility and miscibility of naproxen in poly (vinylpyrrolidone). Mol Pharm. 2010;7:1133–48.
6. Rowe RC, Sheskey PJ, Weller PJ. Handbook of pharmaceutical excipients, 4ed London. UK: Pharmaceutical Press; 2003.
7. Tanno F, Nishiyama Y, Kokubo H, Obara S. Evaluation of hypromellose acetate succinate (HPMCAS) as a carrier in solid dispersions. Drug Dev Ind Pharm. 2004;30:9–17.
8. Sotthivirat S, McKelvey C, Moser J, Rege B, Xu W, Zhang D. Development of amorphous solid dispersion formulations of a poorly water-soluble drug, MK-0364. Int J Pharm. 2013;452:73–81.
9. Ueda K, Higashi K, Yamamoto K, Moribe K. The effect of HPMCAS functional groups on drug crystallization from the supersaturated state and dissolution improvement. Int J Pharm. 2014;464:205–13.
10. Al-Obaidi H, Lawrence MJ, Shah S, Moghul H, Al-Saden N, Bari F. Effect of drug-polymer interactions on the aqueous solubility of milled solid dispersions. Int J Pharm. 2013;446:100–5.
11. Matsumoto T, Zografi G. Physical properties of solid molecular dispersions of indomethacin with poly (vinylpyrrolidone) and poly (vinylpyrrolindone-covinyl-acetate) in relation to indomethacin crystallization. Pharm Res. 1999;16:1722–8.
12. Taylor L, Zografi G. Spectroscopic characterization of interactions between PVP and indomethacin in amorphous molecular dispersions. Pharm Res. 1997;14:1691–8.
13. Konno H, Handa T, Alonzo DE, Taylor LS. Effect of polymer type on the dissolution profile of amorphous solid dispersion containing felodipine. Eur J Pharm Biopharm. 2008;70:493–9.
14. Ilevbare GA, Liu H, Edgar KJ, Taylor LS. Maintaining supersaturation in aqueous drug solutions: impact of different polymers on induction times. Cryst Growth Des. 2013;13:740–51.
15. Qian F, Wang J, Hartley R, Tao J, Haddadin R, Mathias N, *et al.* Solution behavior of PVP-VA and HPMC-AS-based amorphous solid dispersions and their bioavailability implications. Pharm Res. 2012;29:2766–76.
16. Curatolo W, Nightingale JA, Herbig SM. Utility of hydroxypropylmethylcellulose acetate succinate (HPMCAS) for initiation and maintenance of drug supersaturation in the GI milieu. Pharm Res. 2009;26:1419–31.
17. Hiroshi F. Polymer solutions. Amsterdam: Elsevier; 1990.
18. Kamide K. Cellulose and cellulose derivatives: molecular characterization and its applications. San Diego: Elsevier; 2005.
19. Zhong YZ, Wolf P. Effect of hydrophobic unit and its distribution on solution properties of vinylpyrrolidone and vinyl acetate copolymers. J Appl Poly Sci. 1999;74:345–52.
20. Simha R, Weil C. Concerning free volume quantities and the glass temperature. J Macromol Sci-Phys. 1970;4:215–226.
21. Cohen MH, Turnbull D. Molecular transport in liquids and glasses. J Chem Phys. 1959;31:1164–9.
22. Bhardwaj SP, Arora KK, Kwong E, Templeton A, Clas SD, Suryanarayanan R. Correlation between molecular mobility and physical stability of amorphous itraconazole. Mol Pharm. 2013;10: 694–700.
23. Simha R, Somcynsky T. On the statistical thermodynamics of spherical and chain molecule fluids. Macromolecules. 1969;2:342–50.
24. Prigogine I. The molecular theory of solutions. Amsterdam: North Holland Publishing Company; 1957.
25. Moulinié P, Utracki LA. Equation of state and free-volume content. In: Utracki LA, Jamieson AM, editors. Polymer physics: from suspensions to nanocomposites and beyond. Hoboken: Wiley; 2010. p. 227–82.
26. Wästlund C, Maurer FHJ. Positron lifetime distribution and free volume parameters of PEO/PMMA blends determined with the maximum entropy method. Macromolecules. 1997;30:5870–6.
27. Jamieson AM, Olson BG, Nazarenko S. Positron annihilation lifetime studies of free volume in heterogeneous polymer sytems. In: Utracki L, Jamieson AM, editors. Polymer physics: from suspensions to nanocomposites and beyond. Hoboken: Wiley; 2010. p. 473–522.
28. Fang Z, Xu Y, Tong L. Free-volume hole properties of two thermoplastic nanocomposite based on polymer blends probed by positron annihilation lifetime spectroscopy. J Appl Poly Sci. 2006;102:2463–9.
29. Utracki LA. Free volume in molten and glassy polymers and nanocomposites. In: Utracki L, Jamieson AM, editors. Polymer physics: from suspension to nanocomposites and beyond. Hoboken: Wiely; 2010. p. 553–604.
30. Dlubek G, Shaikh MQ, Rätzke K, Pionteck J, Paluch M, Faupel, F. Subnanometer size free volumes in amorphous verapamil hydrochloride: a positron lifetime and PVT study through Tg in comparison with dielectric relaxation spectroscopy. Euro J Pharm Sci. 2010;41:388–98.
31. Bartoš J, Šauša O, Bandzuch P, Zrubcová J, Krištiak J. Free volume factor in supercooled liquid dynamics. J Non-Cryst Solids. 2002;307–310:417–25.
32. Dai GH, Deng Q, Liu J, Shi H, Huang CM, Jean YC. Free-volume hole distribution of polymers by positron annihilation lifetime spectroscopy, Journal de Physique. IV, Colloque, C4 (4th International Workshop on Positron).1993; 233–239.
33. Sato M. Wormlike chain parameters of cellulose and cellulose derivatives. Polym J. 1983;15:213–23.
34. Taghizadeh MT, Foroutan M. A study on P(VP-VA) hydrophobically associating behavior of water-soluble copolymers. Iran Polym J. 2005;14:47–54.
35. Campbell JA, Goodwin AA, Ardi MS, Simon GP, Landry-Coltrain CJT. Free volume studies in miscible polymer blend systems. Macromol Symp. 1997;118:383–8.
36. Van den Mooter G, Wuyts M, Blaton N, Busson R, Grobet P, Augustijns P, *et al.* Physical stabilization of amorphous ketoconazole in solid dispersions with polyvinylpyrrolidone K25. Euro J Pharm Sci. 2001;12:261–9.
37. Zingone G, Moneghini M, Rupena P, Vojnovic D. Characterization and dissolution study of solid dispersions of theophylline and indomethacin with PVP/VA copolymers. S T P Pharm Sci. 1992;2:186–92.
38. Ford JL. The use of thermal analysis in the study of solid dispersions. Drug Dev Ind Pharm. 1987;13:(9):1741–77.
39. Kanaujia P, Lau G, Ng WK, Widjaja E, Hanefeld A, Fischbach M, *et al.* Nanoparticle formation and growth during *in vitro* dissolution of ketoconazole dolid dispersion. J Pharm Sci. 2011;100:2876–85.
40. Yamakawa H. Helical wormlike chains in polymer solutions. New York: Springer; 1997.
41. Kamide K, Saito M. Cellulose and cellulose derivatives: recent advances in physical chemistry. Adv Polym Sci (Biopolymers). 1987;83:1–57.
42. Tao SJ. Positronium annihilation in molecular substances. J Chem Phys. 1972;56:5499–510.
43. Eldrup M, Lightbody D, Sherwood NJ. The temperature dependence of positron lifetimes in solid pivalic acid. Chem Phys. 1981;63: 51–8.

44. Eldrup M, Vehanen A, Schultz PJ, Lynn KG. Positronium formation and diffusion in a molecular solid studied with variable-energy positron. Phys Rev Lett. 1983;51:2007–10.
45. Kwei TK, Pearce EM, Pennacchia JR, Charton M. Correlation between the glass transition temperatures of polymer mixtures and intermolecular forces parameters. Macromolecules. 1987;20:1174–6.
46. Schneider HA, Di Marzio EA. The glass temperature of polymer blends: comparison of both the free volume and the entropy prediction with data. Polymer. 1992;16:3453–61.
47. Liu DS, Shen Q, Ding HG, Zhong L. Influence of the components on Tg of cellulose/poly(ethylene glycol) and model. Xianweisu Kexue Yu Jishu. 2006;14:40–45.